



Article

Assimilation of Satellite-Derived Reservoir Storage Data to Improve Global Hydrodynamic Modeling

Ping Liu ¹, Yulong Ran ¹, Yimeng Zhao ², Zehao Lu ¹, Shufeng Hao ^{1,*}, Shengyu Wang ¹ and Feng Tian ¹

- College of Artificial Intelligence, Taiyuan University of Technology, Taiyuan 030024, China; liuping01@tyut.edu.cn (P.L.); wangshengyv@163.com (S.W.); t854144827@163.com (F.T.)
- ² College of Mechanical Engineering, Taiyuan University of Technology, Taiyuan 030024, China
- * Correspondence: haoshufeng@tyut.edu.cn

Abstract: In this study, we explore the potential of assimilating satellite-derived reservoir storage data into the global-scale hydrodynamic model CaMa-Flood, focusing on the Yangtze River basin. We evaluated three data assimilation (DA) methods: direct assimilation (DIR), anomaly based assimilation (ANO), and normalized assimilation (NOM). Our results show that the DIR method achieved the most significant improvements in reservoir storage and downstream discharge simulations. DIR reduced the average relative root mean square error (rRMSE) of reservoir storage estimates by 80.5%, and increased discharge correlation (Δ CC) by 78.6% in the 14 validated discharge stations. ANO, while effective in certain cases, led to mixed results, with 56.4% of the 39 assimilated dams showing improved storage estimates and a modest 7.8% reduction in average RMSE. NOM had minimal impact, with negligible changes in RMSE or discharge correlation (Δ CC). The direct assimilation method (DIR) consistently outperformed the others, improving both reservoir storage and downstream discharge estimates. However, the magnitude of improvement varied across locations, highlighting the need for the further refinement of DA techniques and input data, especially for regions with complex reservoir operations. Our findings enhance reservoir representation in global hydrodynamic models and improve the predictability of river dynamics and water resource management.

Keywords: data assimilation; satellite data; storage; reservoir; global hydrodynamic model



Citation: Liu, P.; Ran, Y.; Zhao, Y.; Lu, Z.; Hao, S.; Wang, S.; Tian, F.
Assimilation of Satellite-Derived
Reservoir Storage Data to Improve
Global Hydrodynamic Modeling.
Water 2024, 16, 2927. https://doi.org/
10.3390/w16202927

Academic Editor: Bommanna Krishnappan

Received: 19 September 2024 Revised: 9 October 2024 Accepted: 11 October 2024 Published: 15 October 2024



Copyright: © 2024 by the authors. Licensee MDPI, Basel, Switzerland. This article is an open access article distributed under the terms and conditions of the Creative Commons Attribution (CC BY) license (https://creativecommons.org/licenses/by/4.0/).

1. Introduction

Reservoirs are vital components in the global management of water resources, providing essential services for economic, environmental, and social development. They supply water for 30–40% of global irrigation and generate 17% of global electricity [1,2]. The unprecedented surge in reservoir construction has resulted in the damming of many of the world's rivers, significantly impacting river flow regimes at local, regional, and global scales [3,4].

Reservoirs serve multiple functions, including regulating peak flows and hydraulic residence time to mitigate flooding, providing water for agriculture, electricity production, and public consumption, and influencing downstream terrestrial and coastal environments by impeding the flow of essential nutrients [5,6]. However, reservoirs can also emerge as significant sources of greenhouse gas release, adding complexity to their environmental impact [7,8].

Understanding "real river hydrodynamics" necessitates the consideration of dam construction and management practices. Reservoir monitoring and modeling are indispensable prerequisites for advancing our understanding of their impacts on river hydrodynamics and for effective water resource management [9,10]. A key challenge in this field is the lack of publicly available data on reservoir operations, which hinders accurate representation in hydrological models [11,12].

Current approaches to modeling reservoir operations can be broadly categorized into two main types: data-driven and process-based techniques. Data-driven approaches range

Water **2024**, 16, 2927 2 of 17

from simple linear or multilinear regressions to sophisticated artificial intelligence and machine learning algorithms [11,12]. These methods require specific reservoir attributes and access to extensive observed data, limiting their applicability in regions with sparse data. On the other hand, process-based methods conceptualize reservoir response by relating outflow control to real-world physical processes, such as agricultural growth cycles and their corresponding water demands [13,14]. These approaches enable the representation of dam operations without observing actual releases for each reservoir and are often incorporated in global hydrological and water management models. However, they may oversimplify complex reservoir operations [15,16].

Model simulations often exhibit large biases, primarily due to limited observations for calibration and the complex nature of reservoir operations [17,18]. Given these limitations and the scarcity of accessible in situ data, space-based earth observation has become a valuable option for observing reservoirs at global scales [19,20].

Recent developments in remote sensing techniques have the potential to revolutionize reservoir monitoring and modeling. Satellite data can provide water level measurements using altimeters, estimates of reservoir water area from optical imagery, and derived reservoir storage volumes [21,22]. Despite these advancements, satellite data have limitations in accuracy, spatial coverage, and temporal resolution, with gaps spanning days to months between consecutive measurements at given sites [23,24]. These sparse observations may inadequately capture the full scope of reservoir changes.

To address these challenges, data assimilation (DA) offers a solution to integrate remote sensing with sparse observational data and river hydrodynamic models. DA combines models with observations, balancing their uncertainties, to enhance model outputs or replicate the evaluation of real-world systems [25,26]. Previous studies have demonstrated that DA methods can bridge the gap between ground observations and model simulations by leveraging remote sensing data in hydrological applications [27,28].

However, the application of DA techniques to reservoir operations in global hydrodynamic models remains limited. Most existing studies focus on assimilating river water levels or discharge [29,30], while few have explored the assimilation of reservoir storage data derived from satellites. Furthermore, the impact of different DA methods on reservoir storage estimation and downstream flow prediction in global models has not been thoroughly investigated.

In this study, we evaluate the potential of assimilating satellite-based reservoir storage data into a global river hydrodynamic model to facilitate reservoir simulations. Our research goals aim to achieve the following:

- (1) Develop and implement a DA framework for incorporating satellite-derived reservoir storage data into the global river hydrodynamic Catchment-based Macro-scale Floodplain model (CaMa-Flood) [31].
- (2) Compare the performance of different DA methods, including direct, anomaly, and normalized value assimilation.
- (3) Assess the impact of assimilating satellite-based reservoir storage data on down-stream streamflow simulations and reservoir storage simulations.

We investigate these objectives using the Yangtze River basin as our study area, leveraging its extensive network of reservoirs and availability of satellite observations. By addressing these objectives, we aim to contribute to the improvement of global hydrological modeling and enhance our understanding of large-scale reservoir impacts on river systems.

2. Study Area and Data

2.1. Study Area

We have chosen the Yangtze River basin (Figure 1) as a test area for the data assimilation (DA) experiments. The Yangtze River is the world's largest river hydrological system, making it an ideal case study for large-scale hydrodynamic modeling. The Yangtze basin exhibits a wide range of flow dynamics, from seasonal flooding to complex river hydraulics. The basin receives a considerable amount of annual precipitation with a high degree of

Water **2024**, 16, 2927 3 of 17

spatial heterogeneity. It has distinct wet and dry seasons. The Yangtze River basin contains numerous large reservoirs, including the world's largest hydroelectric dam in terms of generated power: the Three Gorges Dam. This extensive network of reservoirs provides an excellent opportunity to study the effect of the operations of reservoirs on river systems at a large scale [32]. The availability of a large number of remote sensing observations is a major advantage for analyzing the Yangtze basin, which is crucial for our DA experiments.

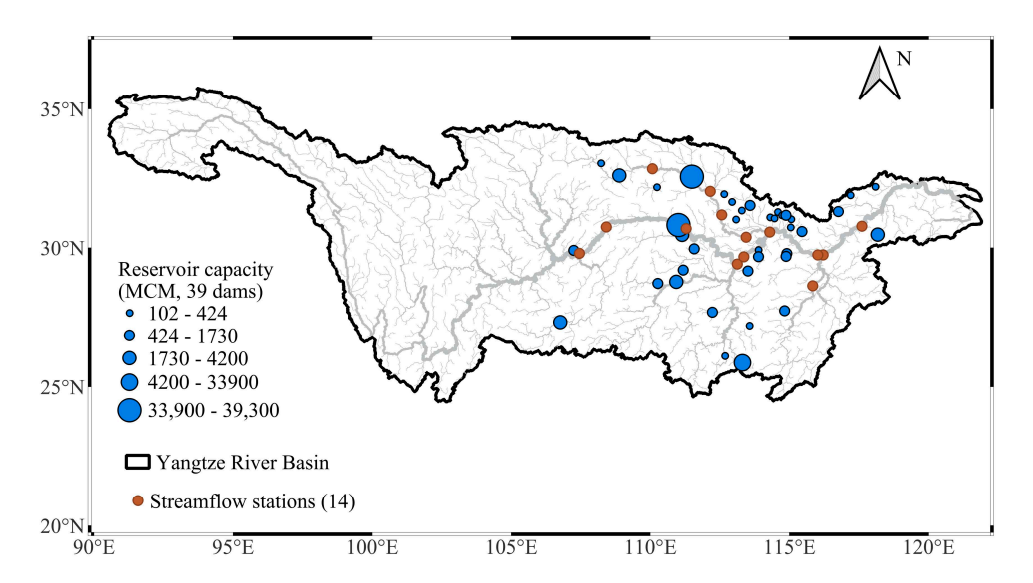


Figure 1. Overview of the study area and datasets used in this study.

2.2. Data

2.2.1. Satellite Reservoir Storage Data

We used satellite-derived reservoir storage data as observations for DA experiments. These data were obtained from Res-CN dataset (https://doi.org/10.5281/zenodo.7664489, accessed on 14 September 2024) [33,34]. The storage estimates from Res-CN are based on satellite-derived water levels, surface water areas, and DEMs (digital elevation models). Satellite-derived water level observations were made using six satellite altimeters: CryoSat-2, ICESat-2, Jason-3, SARAL/AltiKa, and Sentinel-3 A/B. These altimetry data were used in conjunction with surface water areas derived from Landsat and Sentinel-2 images or DEM to generate high-resolution reservoir storage estimates. In situ measurements from 93 reservoirs were used to validate these storage estimates. The comparisons indicate a relatively high level of accuracy of the monthly reservoir storage estimations, with median statistics of 0.89 for the correlation coefficient (CC), 11% for the normalized root mean square error (NRMSE), and 0.021 km³ for the root mean square error (RMSE). Figure 1 illustrates the spatial distribution of the 39 Yangtze reservoirs used in this study.

2.2.2. Validation Data

To evaluate the impact of assimilating satellite reservoir storage on downstream river dynamics, we collected river discharge data from 14 in situ gauging stations located downstream of the reservoirs studied in our study (Figure 1). These in situ measurements serve as independent validation data for our model simulations and DA experiments.

2.2.3. Model Input Data

For the CaMa-Flood model simulations, we used runoff products from the ERA5 to force the model. This dataset was chosen for its global coverage and its relatively high resolution in both space and time. The river network and topography data required by CaMa-Flood were derived from the MERIT Hydro [35]. To allocate reservoirs on the model map, we collected information on the reservoir locations, capacities, and purpose from the Global Reservoir and Dam (GRanD) database [36].

Water **2024**, 16, 2927 4 of 17

3. Methodology

3.1. Data Assimilation Framework

To incorporate satellite reservoir storages into a global river hydrodynamic model, we developed the data assimilation framework HydroDA-Res. The framework (Figure 2) begins with the generation of runoff ensembles through the perturbation of runoff forcing. These ensembles are then used as the input to the CaMa-Flood simulation, which provides the ensembles of current water state (e.g., reservoir storage). Each ensemble of current water state is subsequently corrected through satellite observations in the assimilation scheme.

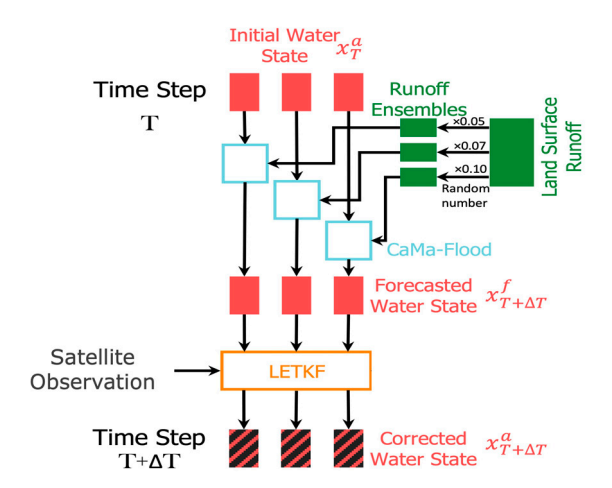


Figure 2. Overview of data assimilation framework (HydroDA-Res) developed in this study.

The process flow of our framework is as follows: The forecasted water state at time $T + \Delta T \left(x_{T+\Delta T}^f \right)$ is simulated with the CaMa-Flood using the initial water state at time $T \left(x_T^a \right)$ and the runoff. The forecasted water state is then modified to $x_{T+\Delta T}^a$ through the DA method, serving as the initial condition for the subsequent calculation step. When employing anomaly based or normalized assimilation approaches, the predicted water conditions undergo a transformation. This process utilizes historical averages and variability measures prior to incorporating adjusted satellite data. Following the assimilation, the updated water states—expressed as deviations from typical values or in standardized units—are reconverted to their original scales. These reconverted values represent the refined estimates of water stored in reservoirs.

3.2. Hydrodynamic Model: CaMa-Flood

We employed the Catchment-based Macro-scale Floodplain model (CaMa-Flood) to simulate reservoir water dynamics within the data assimilation framework. This model is tailored for simulating extensive river systems by dividing global river networks into smaller, manageable units called unit catchments. Its computational efficiency enables accurate flood diagnosis while simultaneously calculating flow and inundation dynamics for each unit catchment, which serves as the basic unit of calculation. The model implements local inertial equations to capture backwater effects and adopts bifurcated channels for the enhanced accuracy of river flow simulations.

In CaMa-Flood, reservoirs are allocated to individual unit catchments based on their geographical locations. The model replaces the natural outflow at the outlet of each unit catchment containing a reservoir by calculating the reservoir outflow based on a reservoir operation scheme. This scheme implements the storage-based rule, which divides the reservoir storage into four zones: dead storage, conservative, normal, and flood control. Each zone has a specific outflow–storage relationship that governs the reservoir's operation. Despite the sophistication of this approach, current simulations of reservoir storage often exhibit large biases when compared to observations. These biases can be attributed to several factors: uncertainties in input data, particularly in estimating mean annual inflow

Water **2024**, 16, 2927 5 of 17

and water demand; simplifications in the reservoir operation rules, which may not capture site-specific management practices; the challenge of representing diverse reservoir purposes and their seasonal variations; and limited information on the actual reservoir characteristics and operations at a global scale.

These features make CaMa-Flood particularly suitable for our DA framework, as it can represent complex hydrodynamic processes at a large scale while providing opportunities for improvement in reservoir storage simulation through data assimilation.

3.3. Data Assimilation Method

The primary goal of DA is to reconcile discrepancies between observed and simulated data by integrating diverse, uncertain information sources. For our research, we selected the Local Ensemble Transform Kalman Filter (LETKF) as our DA methodology. LETKF is a computationally optimized version of the ensemble Kalman filter, which itself is an advanced iteration of the original Kalman filter. This algorithm is frequently employed in scenarios involving nonlinear models, which are essential for accurately representing hydrodynamic processes. The complex nature of hydrodynamic systems necessitates the use of nonlinear models, which can be expressed in a discrete mathematical format as follows:

$$x_{k+1} = \mathbf{M}(x_k, u_k, \vartheta) + q_k \tag{1}$$

where x, u, and ϑ denote the state variable vector, the external model forcing, and the model parameters, respectively. The nonlinear function M describes the system's behavior. The term q_k accounts for a range of potential inaccuracies, including errors in the model forcings, parameters, structures, and antecedent states. Within the vector x, we incorporate all relevant state variables from the CaMa-Flood model, such as river discharge, reservoir storage, and river storage. To link these model states to real-world measurements, we employ the following relationship:

$$y_k = \mathbf{H}(x_k) + \in_k \tag{2}$$

where y and ε denote the observation vector and the vector of errors associated with these observations, respectively. The linear observation operator H establishes a relationship between the model state variables (x) and the observed data (y). For this research, the observations consisted of reservoir storage measurements derived from satellite data. When implementing anomaly based assimilation, both the observed and forecasted states underwent a transformation into anomaly values. The LETKF algorithm was employed to determine the most accurate estimate of the model state vector X, taking into account both the model and observational uncertainties. Here, the model state vector X comprised reservoir storage values. LETKF can be mathematically represented as follows [37]:

$$X^{a} = X^{f} + E^{f} \left[VD^{-1}V^{T} \left(HE^{f} \right)^{T} \left(\frac{R}{w} \right)^{-1} \left(Y^{o} - \overline{HX^{f}} \right) + \sqrt{m-1}VD^{-1/2}V^{T} \right]$$
(3)

where X^a and X^f are the posterior and prior state estimators, respectively; Y^o denotes the observation (i.e., the satellite-derived reservoir storage value); m represents the number of ensemble members; Ef signifies the prior state error covariance, which is directly computed from the perturbations. The uncertainty inherent in the measurements is captured by R, the observation error covariance matrix. To account for spatial relationships, w serves as a weighting factor for observation localization, determined through the semi-variogram analysis of the simulated storage values. VDV^T is expressed as follows:

$$VDV^{T} = (\mathbf{m} - 1)\mathbf{I} + \left(HE^{f}\right)^{T}R^{-1}HE^{f}$$
(4)

where *I* denotes the unit matrix with dimensions m \times m, corresponding to the number of perturbations employed. $VD^{-1}V^T$ and $VD^{-1/2}V^T$ are determined based on eigenvalue

Water **2024**, 16, 2927 6 of 17

decomposition of VDV^T . The ensemble mean vector is indicated by the presence of an overbar symbol.

3.4. Experimental Setup

The first step is to prepare runoff ensembles of the CaMa-Flood. We applied a stochastic modification to each runoff value in the dataset. This modification involved multiplying the original values by random factors drawn from a normal distribution centered at 1 with a standard deviation of 0.1. We created 20 distinct perturbations of the ERA5 runoff product using this method. This approach typically yields a suitable range of runoff forcings for data assimilation experiments, providing a reasonable representation of the uncertainty in the input data.

The second step is to prepare observations and their errors. For anomaly DA experiments, we calculated anomalies values from the long-term (2010–2021) mean and standard deviation of reservoir storage. The statistical parameters for satellite data were computed when the observational records existed, while reservoir simulation statistics were obtained using simulations from 2010 to 2021. We introduced an observed error for each reservoir and used the median of all observed errors as a global value to run the experiments.

Our study encompassed three distinct experimental approaches: direct DA (DIR), anomaly based DA (ANO), and normalized DA (NOM). For the ANO and NOM experiments, we utilized long-term statistics of reservoir storage, specifically the mean and standard deviation calculated over the period from 2010 to 2021. These statistics were used to compute anomalies and normalized values, respectively. In the case of satellite data, we derived the statistical parameters (mean and standard deviation) using the available observational period. Our simulation timeframe extended from 1 January 2010, to 31 December 2021, with the entire year of 2009 serving as a model initialization period to establish stable initial conditions.

3.5. Evaluation

To assess the effectiveness of our assimilation methods, we employed several statistical metrics. These included the Nash–Sutcliffe Efficiency (NSE), the correlation coefficient (CC), the Kling–Gupta Efficiency (KGE), and root mean square error (RMSE). The CC metric was utilized to gauge how well the estimated reservoir storage patterns aligned with seasonal variations. For a comprehensive evaluation of both reservoir storage and flow estimation accuracy, we relied on the NSE and KGE indicators. The RMSE served as our measure of overall discrepancy between the estimated storage/flow values and the observed data. To quantify the benefits of data assimilation, we compared these metrics between the assimilated simulations and the open-loop (non-assimilated) simulations. This comparison allowed us to determine the extent of improvement in both reservoir storage estimates and downstream flow predictions.

4. Results

Our analysis of the three data assimilation (DA) approaches—direct (DIR), anomaly (ANO), and normalized (NOM)—is structured into two main parts: relative performance evaluation and absolute performance evaluation.

4.1. Relative Performance Evaluation

The effectiveness of each data assimilation technique was evaluated by comparing its results to those of the non-assimilated (open-loop) simulation. We use two key metrics: ΔCC for reservoir storage and $\Delta RMSE$ for river discharge. ΔR presents the relative change in correlation coefficient between the DA simulations and the open-loop results. $\Delta RMSE$ shows the relative change in root mean square error, comparing the DA results to the open-loop simulation. These metrics allow us to quantify the improvement (or degradation) in model performance achieved by each DA method compared to the baseline open-loop simulation.

Water **2024**, 16, 2927 7 of 17

4.1.1. Direct Assimilation of Satellite Storage Data

We directly incorporated satellite-derived reservoir storage data into the CaMa-Flood river model. Figure 3a illustrates the change in correlation coefficient (Δ CC) for flow at 14 downstream stations, while Figure 3b shows the relative root mean square error (rRMSE) for reservoir storage at 39 dam locations.

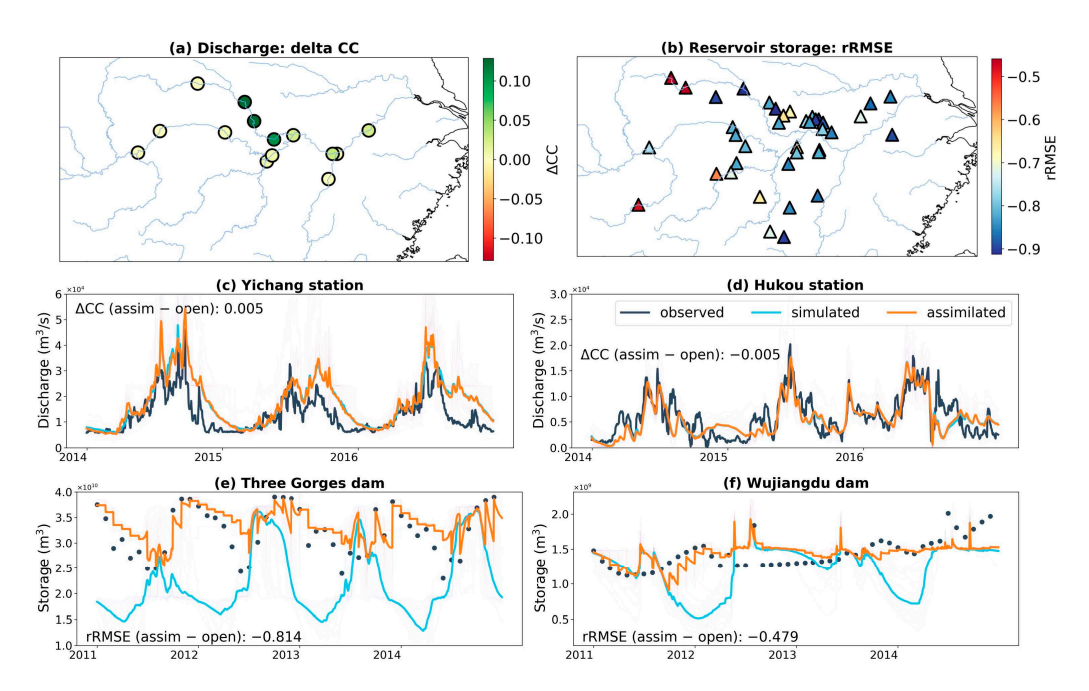


Figure 3. (a) Change in the correlation coefficient (Δ CC) of river flow and (b) the relative root mean square error (rRMSE) in reservoir storage using the DIR method. Hydrographs recorded at Yichang discharge station, Hukou discharge station, Three Gorges dam, and Wujiangdu dam are shown in panels (**c**-**f**), respectively. Blue dots in (**e**,**f**) represent the satellite-derived reservoir storage values.

For river discharge, we observed improvements in the correlation coefficient at 11 out of 14 stations (78.6%). The most significant improvements were seen at Xiangyang ($\Delta CC = 0.13$), Huangzhuang ($\Delta CC = 0.13$), and Xiantao ($\Delta CC = 0.11$). Only three stations showed slight degradations, with Hukou experiencing the largest decrease ($\Delta CC = -0.005$). This suggests that DIR generally enhanced the representation of flow dynamics in the model.

Regarding reservoir storage, all 39 dams showed reductions in RMSE, indicating a consistent improvement in storage estimates. The improvements ranged from moderate (Wujiangdu dam, rRMSE = -0.48) to substantial (Dahongshan dam, rRMSE = -0.96). On average, we observed an 80.5% reduction in RMSE across all dams, demonstrating the effectiveness of DIR in improving reservoir storage simulations.

Figure 3c,d present hydrographs for two representative discharge stations: Yichang and Hukou. At Yichang, we see a slight improvement in correlation ($\Delta CC = 0.0047$), with the assimilated simulation (orange line) more closely matching the observed discharge (black line) compared to the open-loop simulation (blue line). The Hukou station, despite showing a minor decrease in correlation ($\Delta CC = -0.005$), still demonstrates an improved representation of peak flows in the assimilated results.

Figure 3e,f illustrate the storage dynamics at two key dams: Three Gorges and Wujiangdu. The Three Gorges dam shows a significant improvement (rRMSE = -0.81), with the assimilated storage (orange line) capturing the seasonal variations much more accurately than the open-loop simulation (blue line). The Wujiangdu dam, while showing a more moderate improvement (rRMSE = -0.48), still demonstrates better alignment with observed storage patterns after assimilation.

In summary, DIR consistently improved reservoir storage estimates across all studied dams, with an average RMSE reduction of 80.5%. This improvement in storage representa-

Water **2024**, 16, 2927 8 of 17

tion translated to enhanced discharge simulations at most downstream stations, with 78.6% of stations showing increased correlation coefficients. The method proved particularly effective in capturing seasonal variations and improving the representation of peak flows. However, the magnitude of improvement varied across locations, suggesting that local factors such as dam operation rules and basin characteristics play a role in the effectiveness of the assimilation process.

4.1.2. Anomaly Assimilation of Satellite Storage Data

We assimilated the anomalies of satellite-derived reservoir storage into the CaMa-Flood river model for the ANO approach. Figure 4a illustrates the change in correlation coefficient (Δ CC) for flow at 14 downstream stations, while Figure 4b shows the rRMSE for reservoir storage at 39 dam locations.

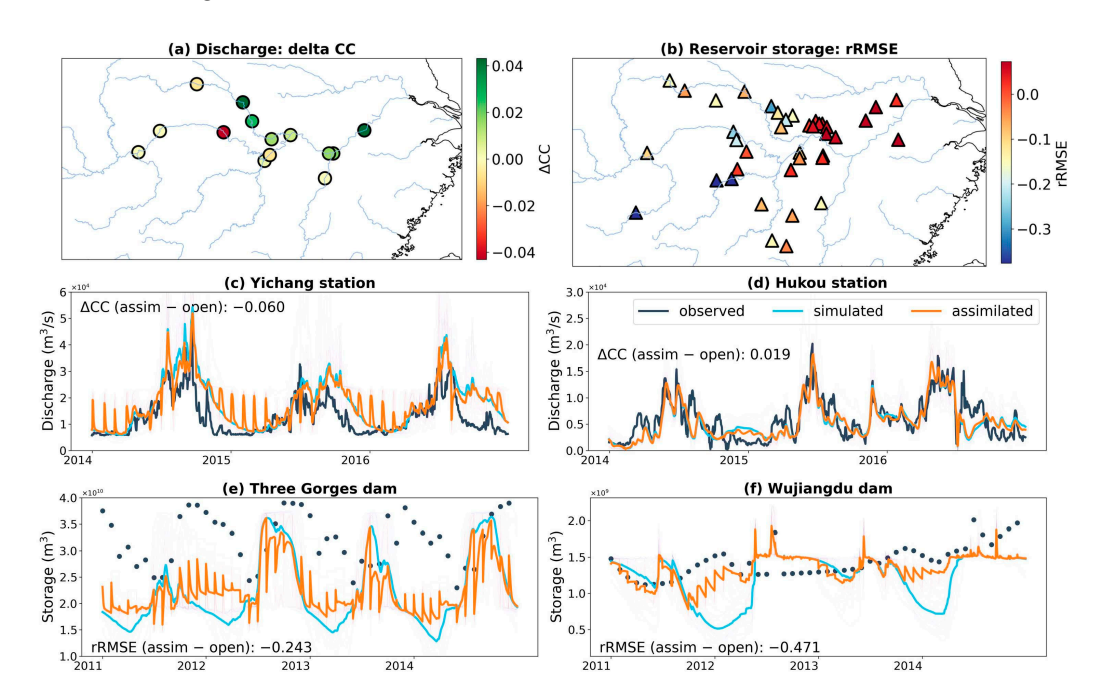


Figure 4. (a) Change in the correlation coefficient (Δ CC) of river flow and (b) the relative root mean square error (rRMSE) in reservoir storage for the ANO method. Hydrographs recorded at Yichang discharge station, Hukou discharge station, Three Gorges dam, and Wujiangdu dam are shown in panels (**c**-**f**), respectively.

For river discharge, we observed improvements in correlation coefficient at 9 out of 14 stations (64.3%). The most notable improvements were seen at Datong ($\Delta CC = 0.043$), Xiangyang ($\Delta CC = 0.044$), and Huangzhuang ($\Delta CC = 0.03$). However, five stations showed slight degradations, with Yichang experiencing the largest decrease ($\Delta CC = -0.0601$). This suggests that ANO generally enhanced the representation of flow dynamics, but not as consistently as the DIR method.

Regarding reservoir storage, 22 out of 39 dams (56.4%) showed reductions in RMSE, indicating an improvement in storage estimates for the majority of locations. The improvements ranged from slight (Weishui dam, rRMSE = -0.0001) to substantial (Wujiangdu dam, rRMSE = -0.47). However, 17 dams showed increased RMSE, with Niuchehe dam experiencing the largest increase (rRMSE = 0.10). On average, we observed a 7.8% reduction in RMSE across all dams, demonstrating a modest overall improvement in reservoir storage simulations with the ANO method.

Figure 4c,d present hydrographs for two representative discharge stations: Yichang and Hukou. At Yichang, we see a degradation in correlation ($\Delta CC = -0.06$), with the assimilated simulation (orange line) deviating from the observed discharge (black line) more than the open-loop simulation (blue line) in some periods. However, the Hukou

Water **2024**, 16, 2927 9 of 17

station shows an improvement in correlation ($\Delta CC = 0.02$), with the assimilated results better capturing the overall discharge patterns, particularly during low flow periods.

Figure 4e,f illustrate the storage dynamics at two key dams: Three Gorges and Wujiangdu. The Three Gorges dam shows a notable improvement (rRMSE = -0.24), with the assimilated storage (orange line) better capturing the seasonal variations compared to the open-loop simulation (blue line), especially during drawdown periods. The Wujiangdu dam demonstrates an even more significant improvement (rRMSE = -0.4711), with the assimilated results closely aligning with observed storage patterns throughout the simulation period.

In summary, the ANO method showed mixed results, with improvements in 64.3% of discharge stations and 56.4% of dam storage simulations. The average RMSE reduction of 7.8% for reservoir storage, while positive, is less substantial than that achieved by the DIR method. The ANO approach proved particularly effective in improving storage estimates for some large dams like Three Gorges and Wujiangdu, and in enhancing discharge simulations at stations like Datong and Xiangyang. However, the variability in results suggests that the effectiveness of the ANO method may be more sensitive to local conditions and the specific characteristics of each reservoir and river reach. The method's performance in capturing seasonal variations and improving low flow representations was notable in some cases, but it also led to degradations in others, highlighting the complexity of applying anomaly based assimilation in diverse hydrological settings.

4.1.3. Normalized Assimilation of Satellite Storage Data

We assimilated normalized satellite-derived reservoir storage data into the CaMa-Flood river model for the NOM method. Figure 5a illustrates the change in correlation coefficient (Δ CC) for flow at 14 downstream stations, while Figure 5b shows the rRMSE for reservoir storage at 39 dam locations.

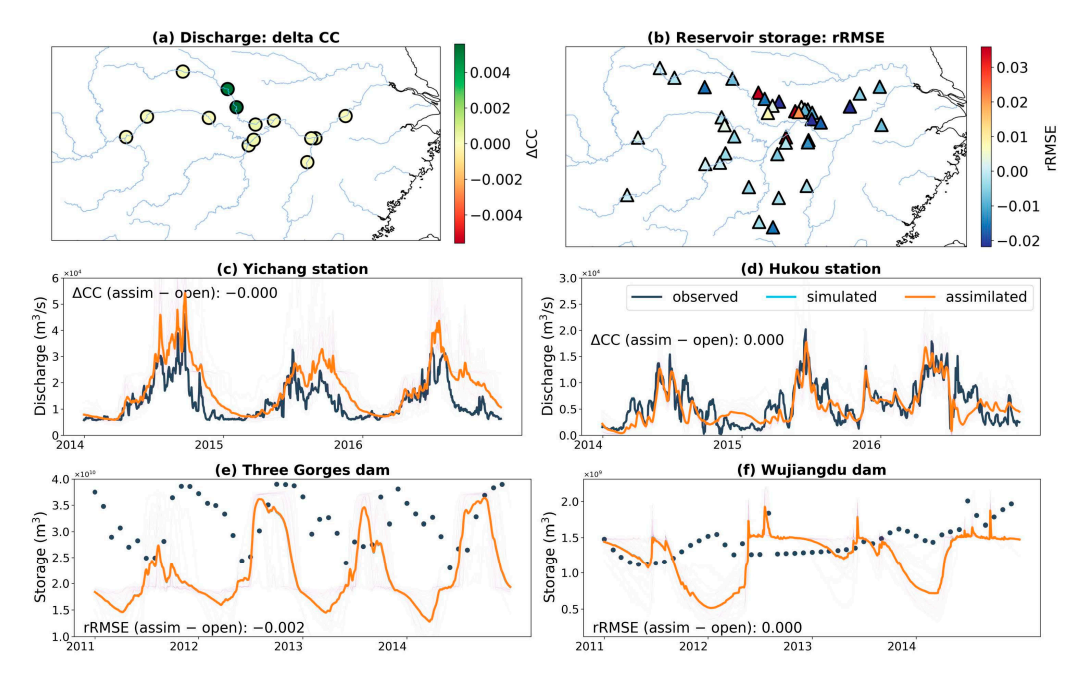


Figure 5. (a) Change in the correlation coefficient (Δ CC) of river flow and (b) the relative root mean square error (rRMSE) in reservoir storage for the NOM method. Hydrographs recorded at Yichang discharge station, Hukou discharge station, Three Gorges dam, and Wujiangdu dam are shown in panels (c-f), respectively.

For river discharge, we observed minimal changes in correlation coefficients across all 14 stations. The largest improvements were seen at Huangzhuang ($\Delta CC = 0.006$) and Xiangyang ($\Delta CC = 0.005$), while the largest degradation was at Yichang ($\Delta CC = -0.00002$).

Water **2024**, 16, 2927 10 of 17

These changes are extremely small, indicating that the NOM method had very little impact on the temporal patterns of discharge simulations.

Regarding reservoir storage, 24 out of 39 dams (61.5%) showed reductions in RMSE, indicating a slight improvement in storage estimates for the majority of locations. The improvements were generally minor, with the largest reduction seen at Longhekou dam (rRMSE = -0.02). Conversely, some dams showed increased RMSE, with Xionghe dam experiencing the largest increase (rRMSE = 0.32). On average, we observed a 0.3% reduction in RMSE across all dams, demonstrating a very modest overall improvement in reservoir storage simulations with the NOM method.

Figure 5c,d present hydrographs for two representative discharge stations: Yichang and Hukou. At both stations, the assimilated simulation (orange line) is nearly indistinguishable from the open-loop simulation (blue line), confirming the minimal impact of the NOM method on discharge simulations. This is reflected in the Δ CC values of -0.00002 for Yichang and 0.00018 for Hukou.

Figure 5e,f illustrate the storage dynamics at two key dams: Three Gorges and Wujiangdu. The Three Gorges dam shows a very slight improvement (rRMSE = -0.002), with the assimilated storage (orange line) barely differing from the open-loop simulation (blue line). The Wujiangdu dam demonstrates an even smaller change (rRMSE = 0.00035), with the assimilated results closely mirroring those of the non-assimilated model across the entire simulated period.

In summary, the NOM method showed minimal impact on both discharge and reservoir storage simulations. The average RMSE reduction of 0.3% for reservoir storage is negligible, and the changes in discharge correlation coefficients are extremely small. While the method did lead to slight improvements in more than half of the dam storage simulations, these improvements were not substantial enough to significantly alter the overall model performance.

4.1.4. Comparison of Assimilation Experiments

In our assessment of the effectiveness of various DA techniques, we examined two key performance indicators across three experimental setups: DIR, ANO, and NOM. For reservoir storage, we quantified improvements using the relative change in root mean square error (rRMSE). Concurrently, we gauged enhancements in downstream flow predictions by measuring shifts in correlation coefficients (Δ CC).

Figure 6a displays boxplots of the rRMSE for reservoir storage across the 39 dams for each experiment. The DIR experiment showed the most significant improvement, with a median rRMSE of approximately -0.8, indicating a substantial reduction in RMSE compared to the open-loop simulation. The interquartile range for DIR is also the largest, suggesting variability in the degree of improvement across different reservoirs. The ANO experiment showed moderate improvement, with a median rRMSE around -0.1, while the NOM experiment demonstrated minimal change, with its median rRMSE close to zero.

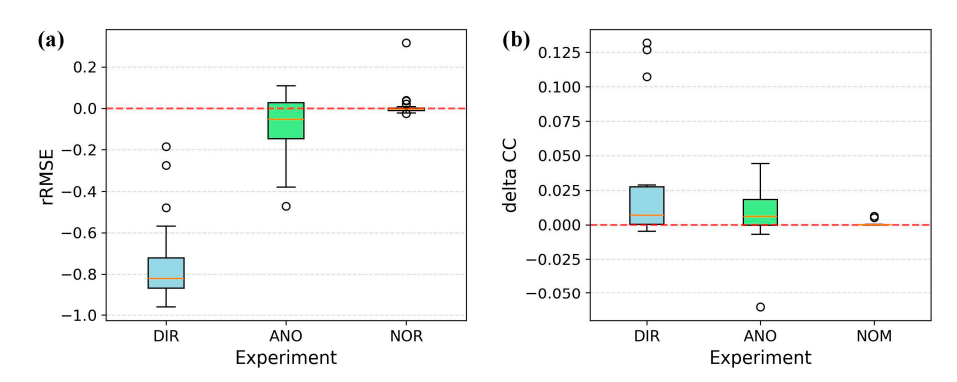


Figure 6. Boxplots of (a) the delta correlation coefficient (Δ CC) and (b) the relative change RMSE (rRMSE) for each experiment (i.e., DIR, ANO, and NOM experiments).

Water **2024**, 16, 2927 11 of 17

For downstream discharge, Figure 6b illustrates the ΔCC across the 14 discharge stations. The DIR experiment again showed the largest improvement, with a median ΔCC of about 0.02, indicating a slight increase in correlation between the simulated and observed discharge. The ANO experiment showed a smaller but still positive median ΔCC , while the NOM experiment resulted in minimal changes, with its median ΔCC very close to zero.

The DIR experiment consistently outperformed the other methods in both reservoir storage and discharge simulations. It led to substantial improvements in reservoir storage estimates and modest enhancements in discharge correlations. The ANO experiment showed moderate benefits, particularly in reservoir storage, but its improvements were less pronounced than DIR. The NOM experiment, while maintaining model stability, did not significantly alter the model's performance relative to the open-loop results.

These results suggest that the direct assimilation of satellite-derived reservoir storage data is the most effective approach for improving both reservoir operation representations and downstream discharge simulations in the CaMa-Flood for the Yangtze River basin. DIR method's superior performance may be attributed to its ability to make more substantial adjustments to the model states, leveraging the satellite observations more effectively than the other methods.

However, it is important to note that while DIR showed the largest improvements, it also exhibited the greatest variability in results, as evidenced by the wider interquartile ranges in both rRMSE and Δ CC. This suggests that the effectiveness of direct assimilation may vary significantly across different reservoirs and discharge stations, possibly due to factors such as reservoir size, operation complexity, or data quality.

In conclusion, based on the rRMSE for reservoir storage and ΔCC for discharge, the direct assimilation method (DIR) emerges as the most effective approach for improving the CaMa-Flood model's performance in the Yangtze River basin, followed by the anomaly method (ANO), while the normalized method (NOM) offers minimal improvements but maintains model stability.

4.2. Absolute Performance Evaluation

Our analysis now shifts to evaluating the absolute accuracy of our model's predictions for river flow and reservoir water volumes. To quantify river discharge performance, we utilize a trio of statistical indicators: CC, NSE, and KGE. For assessing reservoir storage precision, we rely on the RMSE metric.

4.2.1. Estimation of Downstream Discharge

Figure 7 illustrates the spatial distribution of these metrics for each experiment. In the DIR experiment (Figure 7, top row), we observed generally good performance across the basin. The correlation coefficients were consistently high, with 11 out of 14 stations (78.6%) showing a CC > 0.8 and a median CC of 0.89. The highest CC was observed at Waizhou (0.91) and Luoshan (0.89). NSE values showed more variability, with a median of 0.45. The best NSE performance was seen at Waizhou (0.77) and Luoshan (0.75), while some stations like Xiantao (0.14) and Xiangyang (0.05) showed lower efficiency. KGE values were generally good, with a median of 0.62. The highest KGE was observed at Chenglingji (0.82) and Baihe (0.71).

The ANO experiment (Figure 7, middle row) showed similar performance to DIR in terms of correlation, but with some improvements in NSE and KGE for certain stations. The median CC remained high at 0.88, with 11 stations (78.6%) showing a CC > 0.8. The NSE values improved for some stations, with a median of 0.49. Notable improvements were seen at Datong (NSE increased from 0.39 to 0.45) and Hankou (from 0.35 to 0.4). The KGE values were comparable to DIR, with a median of 0.61.

The NOM experiment (Figure 7, bottom row) showed slight decreases in performance compared to DIR and ANO, but still maintained good overall results. The median CC was 0.89, with 11 stations (78.6%) having a CC > 0.8, similar to the other experiments. NSE

Water **2024**, 16, 2927

values showed a slight decrease, with a median of 0.43. KGE values also showed a minor decrease, with a median of 0.60.

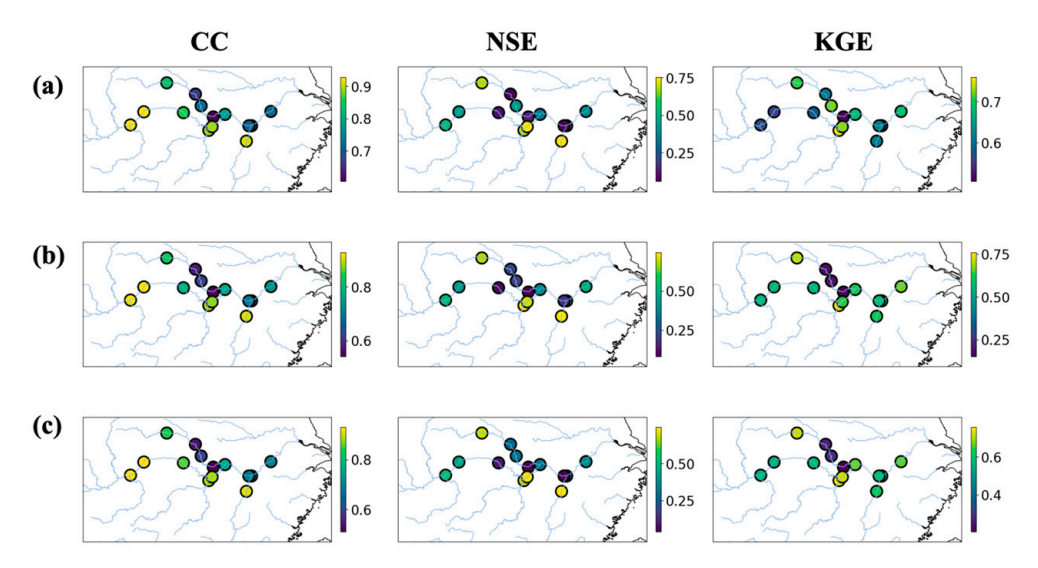


Figure 7. Evaluation of daily river flow accuracy using three statistical metrics: Nash–Sutcliffe efficiency (NSE), correlation coefficient (CC), and Kling–Gupta efficiency (KGE) across three DA methods: (a) DIR, (b) ANO, and (c) NOM.

Across all experiments, certain stations consistently performed well. Waizhou and Luoshan maintained high performance across all metrics and experiments. Conversely, stations like Xiantao and Xiangyang showed lower performance across all experiments, suggesting local factors may be affecting model performance in these areas.

In summary, all three DA methods demonstrated good performance in estimating river discharge, with DIR and ANO showing slightly better results than NOM. The high correlation coefficients across all experiments demonstrate that the temporal dynamics of flow are well captured. The variability in NSE and KGE values suggests that while the overall patterns are well represented, there is room for improvement in capturing the magnitude and variability of discharge at some stations. The spatial distribution of performance metrics highlights the complexity of the Yangtze River basin, with varying levels of DA effectiveness across different regions.

4.2.2. Estimation of Daily Reservoir Storage

We accessed the performance of daily reservoir storage estimates across the DIR, ANO, and NOM data assimilation experiments for 39 Yangtze dams. Figure 8 illustrates the geographic distribution of RMSE for each experiment.



Figure 8. RMSE values of reservoir storage simulations across three DA methods: (a) DIR, (b) ANO, and (c) NOM.

In the DIR experiment (Figure 8a), we observed generally lower RMSE values compared to the other methods, indicating better performance. The RMSE values ranged from 3.06×10^6 m³ (Dahongshan dam) to 2.35×10^9 m³ (Three Gorges Dam). The median RMSE was approximately 2.50×10^7 m³. Notably, smaller dams like Huohe (5.96×10^6 m³) and Niuchehe (9.20×10^6 m³) showed very low RMSE, while larger reservoirs like Danjiangkou

Water **2024**, 16, 2927 13 of 17

 $(1.60 \times 10^9 \text{ m}^3)$ and Three Gorges Dam $(2.35 \times 10^9 \text{ m}^3)$ had higher absolute RMSE values, which is expected given their larger storage capacities.

The ANO experiment (Figure 8b) showed mixed results compared to DIR. Some dams saw improvements, while others experienced an increased RMSE. The RMSE values ranged from 1.76×10^7 m³ (Sanhulianjiang dam) to 9.55×10^9 m³ (Three Gorges Dam). The median RMSE was around 3.75×10^8 m³, higher than in the DIR experiment. Notably, the Three Gorges Dam showed a significant increase in RMSE (9.55×10^9 m³) compared to DIR, suggesting that the anomaly method may struggle with very large reservoirs.

The NOM experiment (Figure 8c) generally showed higher RMSE values compared to DIR but performed better than ANO for some dams. RMSE values ranged from 4.20×10^7 m³ (Niuchehe dam) to 1.74×10^{10} m³ (Danjiangkou dam). The median RMSE was approximately 4.35×10^8 m³. Interestingly, while the Three Gorges Dam showed improvement compared to ANO (1.26×10^{10} m³), it still had higher RMSE than in the DIR experiment.

Across all of the three methods, we observed that DIR generally performed best, with lower RMSE values for most dams. ANO showed mixed results, with some dams improving and others degrading compared to DIR. NOM typically had higher RMSE values than DIR but showed improvements over ANO for several dams. The performance varied significantly across different dam sizes. Smaller dams often had lower absolute RMSE values, while larger dams like Three Gorges and Danjiangkou consistently showed higher RMSE across all methods due to their larger storage capacities.

In conclusion, the direct assimilation method appears to be the most effective for estimating the daily storage of the Yangtze's reservoirs. However, the performance of each method varies across different dam sizes and locations, suggesting that local factors and reservoir characteristics play a significant role in the effectiveness of these data assimilation techniques. Future work could focus on understanding these local factors to improve estimation accuracy, particularly for larger reservoirs.

5. Discussion

5.1. Effectiveness of Different DA Methods for Reservoir Storage Assimilation

Our study compared three data assimilation (DA) methods—Direct (DIR), Anomaly (ANO), and Normalized (NOM)—for integrating satellite-derived reservoir storage observations into the CaMa-Flood river model. The results highlight the superior performance of the DIR method, which generally outperformed both ANO and NOM in improving reservoir storage estimates. The DIR method's advantage is primarily due to its direct integration of observed values without data transformation, making it more effective in matching the model's storage predictions with satellite-derived observations.

However, the ANO and NOM methods rely on transforming the data before assimilation, such as by calculating anomalies or normalizing values, which can introduce inaccuracies when the temporal resolution of the satellite observations is sparse. This transformation might struggle to account for the temporal variability inherent in reservoir operations, particularly in regions where reservoir inflows and outflows vary due to both natural hydrological processes and human intervention. For instance, reservoirs with nonlinear or unpredictable operational behavior pose a significant challenge to anomaly based or normalized DA methods.

Furthermore, in some cases, the ANO and NOM methods led to a degraded performance, underscoring that not all transformation-based DA techniques are universally suitable. The discrepancy between the transformed dataset and actual reservoir management practices indicates a need for further investigation. Future studies should prioritize the development of more flexible data assimilation methods. These advanced techniques should be capable of reconciling the limitations in satellite data frequency with the complex operational dynamics of reservoir systems.

Water **2024**, 16, 2927 14 of 17

5.2. Limitations of Current Hydrodynamic Models in Reservoir Representation

While improvements were observed in reservoir storage estimates through DA, down-stream discharge simulations showed limited enhancement. This result exposes a crucial limitation of global hydrodynamic models like CaMa-Flood: their inability to accurately capture reservoir dynamics and their effects on river systems. Reservoirs play a complex role in modifying downstream flow regimes by buffering inflows, regulating discharge patterns, and storing water for operational purposes such as power generation and flood control.

One primary limitation of hydrodynamic models is the simplification of reservoir operation rules. Most large-scale models rely on generalized assumptions that may fail to reflect the diverse strategies employed by water managers, who adjust reservoir operations based on seasonal variations, downstream needs, and socio-economic factors. Consequently, the mismatch between modeled and real-world reservoir behavior leads to discrepancies in simulated downstream discharges.

Additionally, models often lack detailed information about reservoir characteristics such as depth–area–volume relationships, spillway configurations, and operational rules [38,39]. Without these details, models cannot accurately simulate how reservoirs respond to incoming flows, particularly during extreme events like floods or droughts. Moreover, the interaction between reservoirs and surrounding hydrological systems, such as feedback mechanisms with groundwater or regional climate patterns, is typically oversimplified. These gaps highlight the need for enhanced modeling approaches that incorporate dynamic and real-world reservoir management strategies.

5.3. Influence of Model and Data Quality on DA Performance

Our findings reveal that the success of DA methods is closely tied to the quality of both the model inputs and the assimilated satellite data. In particular, we identified three critical factors influencing DA performance: the accuracy of runoff data, river bathymetry, and satellite observation characteristics.

First, biased runoff data can severely impact DA outcomes. When the input runoff to the hydrodynamic model is inaccurate or contains biases, even the most effective DA method may fail to correct the model's errors. For instance, inflow patterns that are incorrectly timed or overestimated can lead to suboptimal reservoir storage estimates, regardless of the DA technique used. Therefore, improving the accuracy of hydrological inputs, particularly runoff, is essential for optimizing DA methods.

Second, errors in river bathymetry, especially inaccuracies in cross-sectional profiles, can undermine the ability of DA to improve discharge simulations. Since the geometry of a river channel determines its flow characteristics, inaccuracies in channel depth or width can cause the model to misestimate the flow velocity and water storage. Severe bathymetry errors may even render DA efforts ineffective, as the model will struggle to simulate realistic river hydraulics.

Finally, the temporal and spatial resolution of satellite observations is pivotal. Higher resolution data allow DA methods to better capture short-term variations in reservoir storage, which is particularly important for regions with high hydrological variability or rapidly changing storage conditions. However, when satellite data are sparse or have low temporal resolution, DA methods struggle to make meaningful adjustments, especially for reservoirs with complex operational patterns. Addressing these data quality issues will be essential to maximize the effectiveness of DA in large-scale hydrodynamic models.

6. Conclusions

This study demonstrates the potential for assimilating satellite-derived reservoir storage data into hydrodynamic models to improve the representation of reservoir behavior in large river systems. Among the three DA methods tested, the direct assimilation (DIR) method showed the most promise, outperforming the anomaly (ANO) and normalized (NOM) approaches. The DIR method's ability to directly integrate observed storage data

Water **2024**, 16, 2927 15 of 17

without the need for transformation allowed it to more effectively align with the model's predictions, resulting in better reservoir storage estimates.

However, our results also highlight ongoing challenges, particularly in simulating downstream discharge influenced by reservoirs. The limited improvement in discharge simulations underscores the need for more sophisticated reservoir representation in hydrodynamic models. Future work should focus on developing dynamic reservoir operation schemes that better reflect real-world management practices, improving the quality and resolution of model inputs (e.g., runoff, bathymetry), and refining satellite observations.

Moreover, exploring advanced DA techniques that can account for the unique characteristics of reservoir systems, such as their varying operational strategies and interactions with broader hydrological processes, will be crucial. Investigating how improvements in reservoir storage estimates propagate downstream, influencing river discharge and flood risk, is another essential area for future research. By addressing these challenges, we can enhance our ability to model large river systems, leading to better water resource management and flood prediction in reservoir-influenced basins.

Author Contributions: Conceptualization, P.L.; methodology, Y.R. and S.H.; software, Z.L.; validation, Y.R., Y.Z. and S.H.; formal analysis, Y.Z. and S.W.; investigation, F.T.; resources, P.L.; data curation, Z.L.; writing—original draft, Y.R. and Z.L.; writing—review and editing, P.L., Y.R. and Y.Z.; visualization, S.W.; supervision, P.L. and S.H.; project administration, P.L.; funding acquisition, P.L. All authors have read and agreed to the published version of the manuscript.

Funding: This work was supported in part by the Key R&D Projects in Shanxi Province under Grant No. 202202020101007, the Fundamental Research Programs of Shanxi Province under Grant No. 20210302124168, the Fund Program for the Scientific Activities of Selected Returned Overseas Professionals in Shanxi Province under Grant No. 20220009, and the Key R&D Projects in Shanxi Province under Grant No. 202102020101004.

Data Availability Statement: Datasets are openly accessible from the link provided in the main texts or the cited references.

Acknowledgments: We acknowledge Menaka Revel for sharing some valuable codes.

Conflicts of Interest: The authors declare no conflicts of interest.

References

- 1. Intralawan, A.; Wood, D.; Frankel, R.; Costanza, R.; Kubiszewski, I. Tradeoff analysis between electricity generation and ecosystem services in the lower Mekong Basin. *Ecosyst. Serv.* **2018**, *30*, 27–35. [CrossRef]
- 2. Boulange, J.; Hanasaki, N.; Yamazaki, D.; Pokhrel, Y. Role of dams in reducing global flood exposure under climate change. *Nat. Commun.* **2021**, *12*, 417. [CrossRef] [PubMed]
- 3. Grill, G.; Lehner, B.; Lumsdon, A.E.; MacDonald, G.K.; Zarfl, C.; Liermann, C.R. An index-based framework for assessing patterns and trends in river fragmentation and flow regulation by global dams at multiple scales. *Environ. Res. Lett.* **2015**, *10*, 015001. [CrossRef]
- 4. Grill, G.; Lehner, B.; Thieme, M.; Geenen, B.; Tickner, D.; Antonelli, F.; Babu, S.; Borrelli, P.; Cheng, L.; Crochetiere, H.; et al. Mapping the world's free-flowing rivers. *Nature* **2019**, *569*, 215–221. [CrossRef]
- 5. Li, R.; Xiong, L.; Xiong, B.; Li, Y.; Xu, Q.; Cheng, L.; Xu, C.-Y. Investigating the downstream sediment load change by an index coupling effective rainfall information with reservoir sediment trapping capacity. *J. Hydrol.* **2020**, *590*, 125200. [CrossRef]
- 6. Maavara, T.; Chen, Q.; Van Meter, K.; Brown, L.E.; Zhang, J.; Ni, J.; Zarfl, C. River dam impacts on biogeochemical cycling. *Nat. Rev. Earth Environ.* **2020**, *1*, 103–116. [CrossRef]
- 7. Abbott, B.W.; Bishop, K.; Zarnetske, J.P.; Minaudo, C.; Chapin, F.S., III; Krause, S.; Hannah, D.M.; Conner, L.; Ellison, D.; Godsey, S.E.; et al. Human domination of the global water cycle absent from depictions and perceptions. *Nat. Geosci.* **2019**, *12*, 533–540. [CrossRef]
- 8. Veldkamp, T.I.E.; Zhao, F.; Ward, P.J.; de Moel, H.; Aerts, J.C.; Schmied, H.M.; Portmann, F.T.; Masaki, Y.; Pokhrel, Y.; Liu, X.; et al. Human impact parameterizations in global hydrological models improve estimates of monthly discharges and hydrological extremes: A multi-model validation study. *Environ. Res. Lett.* **2019**, *13*, 055008. [CrossRef]
- 9. Tavakoly, A.A.; Gutenson, J.L.; Lewis, J.W.; Follum, M.L.; Rajib, A.; La Hatte, W.C.; Hamilton, C.O. Direct integration of numerous dams and reservoirs outflow in continental scale hydrologic modeling. *Water Resour. Res.* **2021**, *57*, e2020WR029544. [CrossRef]
- 10. Wang, Y.; Li, J.; Zhang, T.; Wang, B. Changes in drought propagation under the regulation of reservoirs and water diversion. *Theor. Appl. Climatol.* **2019**, *138*, 701–711. [CrossRef]

Water **2024**, 16, 2927 16 of 17

11. Yassin, F.; Razavi, S.; Elshamy, M.; Davison, B.; Sapriza-Azuri, G.; Wheater, H. Representation and improved parameterization of reservoir operation in hydrological and land-surface models. *Hydrol. Earth Syst. Sci.* **2019**, 23, 3735–3764. [CrossRef]

- 12. Neitsch, S.L.L.; Arnold, J.G.G.; Kiniry, J.R.R.; Williams, J.R.R. *Soil and Water Assessment Tool Theoretical Documentation*; Texas Water Resources Institute Technical Report; Texas Water Resources Institute: College Station, TX, USA, 2005.
- 13. Wu, Y.; Chen, J. An Operation-Based Scheme for a Multiyear and Multipurpose Reservoir to Enhance Macroscale Hydrologic Models. *J. Hydrometeorol.* **2012**, *13*, 270–283. [CrossRef]
- 14. Van der Sande, C.J.; De Jong, S.M.; De Roo, A.P.J. A segmentation and classification approach of IKONOS-2 imagery for land cover mapping to assist flood risk and flood damage assessment. *Int. J. Appl. Earth Obs. Geoinf.* **2003**, *4*, 217–229. [CrossRef]
- 15. Burek, P.; van der Knijff, J.; de Roo, A. LISFLOOD Distributed Water Balance and Flood Simulation Model—Revised User Manual 2013; JRC Technical Reports; Joint Research Centre of the European Commission: Luxembourg, 2013.
- Hanasaki, N.; Yoshikawa, S.; Pokhrel, Y.; Kanae, S. A global hydrological simulation to specify the sources of water used by humans. Hydrol. Earth Syst. Sci. 2018, 22, 789–817. [CrossRef]
- 17. Bernhofen, M.V.; Whyman, C.; Trigg, M.A.; Sleigh, P.A.; Smith, A.M.; Sampson, C.C.; Yamazaki, D.; Ward, P.J.; Rudari, R.; Pappenberger, F.; et al. A first collective validation of global fluvial flood models for major floods in Nigeria and Mozambique. *Environ. Res. Lett.* **2018**, 13, 104007. [CrossRef]
- 18. Hirpa, F.A.; Lorini, V.; Dadson, S.J.; Salamon, P. Calibration of Global Flood Models. In *Global Drought and Flood: Observation, Modeling, and Prediction*; American Geophysical Union: Washington, DC, USA, 2021; pp. 201–211. [CrossRef]
- 19. Liu, K.; Song, C.; Wang, J.; Ke, L.; Zhu, Y.; Zhu, J.; Ma, R.; Luo, Z. Remote sensing-based modeling of the bathymetry and water storage for channel-type reservoirs worldwide. *Water Resour. Res.* **2020**, *56*, e2020WR027147. [CrossRef]
- 20. Bonnema, M.; Hossain, F. Assessing the potential of the Surface Water and Ocean Topography Mission for reservoir monitoring in the Mekong River basin. *Water Resour. Res.* **2019**, *55*, 444–461. [CrossRef]
- 21. Khandelwal, A.; Karpatne, A.; Ravirathinam, P.; Ghosh, R.; Wei, Z.; Dugan, H.A.; Hanson, P.C.; Kumar, V. ReaLSAT, a global dataset of reservoir and lake surface area variations. *Sci. Data* **2022**, *9*, 356. [CrossRef]
- 22. Zhao, G.; Gao, H. Automatic Correction of Contaminated Images for Assessment of Reservoir Surface Area Dynamics. *Geophys. Res. Lett.* **2018**, *45*, 6092–6099. [CrossRef]
- 23. Donchyts, G.; Winsemius, H.; Baart, F.; Dahm, R.; Schellekens, J.; Gorelick, N.; Iceland, C.; Schmeier, S. High-resolution surface water dynamics in Earth's small and medium-sized reservoirs. *Sci. Rep.* **2022**, *12*, 13776. [CrossRef]
- 24. Klein, I.; Mayr, S.; Gessner, U.; Hirner, A.; Kuenzer, C. Water and hydropower reservoirs: High temporal resolution time series derived from MODIS data to characterize seasonality and variability. *Remote Sens. Environ.* **2021**, 253, 112207. [CrossRef]
- 25. Emery, C.M.; Biancamaria, S.; Boone, A.; Ricci, S.; Rochoux, M.C.; Pedinotti, V.; David, C.H. Assimilation of wide-swath altimetry water elevation anomalies to correct large-scale river routing model parameters. *Hydrol. Earth Syst. Sci.* **2020**, 24, 2207–2233. [CrossRef]
- 26. Michailovsky, C.I.; Milzow, C.; Bauer-Gottwein, P. Assimilation of radar altimetry to a routing model of the Brahmaputra River. *Water Resour. Res.* **2013**, *49*, 4807–4816. [CrossRef]
- 27. Paiva, R.C.D.; Collischonn, W.; Bonnet, M.-P.; de Gonçalves, L.G.G.; Calmant, S.; Getirana, A.; Santos da Silva, J. Assimilating in situ and radar altimetry data into a large-scale hydrologic-hydrodynamic model for streamflow forecast in the Amazon. *Hydrol. Earth Syst. Sci.* **2013**, *17*, 2929–2946. [CrossRef]
- 28. Revel, M.; Ikeshima, D.; Yamazaki, D.; Kanae, S. A Physically Based Empirical Localization Method for Assimilating Synthetic SWOT Observations of a Continental-Scale River: A Case Study in the Congo Basin. *Water* **2019**, *11*, 829. [CrossRef]
- 29. Revel, M.; Ikeshima, D.; Yamazaki, D.; Kanae, S. A Framework for Estimating Global-Scale River Discharge by Assimilating Satellite Altimetry. *Water Resour. Res.* **2021**, 57, e2020WR027876. [CrossRef]
- 30. Yoon, Y.; Durand, M.; Merry, C.J.; Clark, E.A.; Andreadis, K.M.; Alsdorf, D.E. Estimating river bathymetry from data assimilation of synthetic SWOT measurements. *J. Hydrol.* **2012**, *464*–*465*, 363–375. [CrossRef]
- 31. Yamazaki, D.; Kanae, S.; Kim, H.; Oki, T. A physically based description of floodplain inundation dynamics in a global river routing model. *Water Resour. Res.* **2011**, 47, W04501. [CrossRef]
- 32. Liu, D.; Guo, S.; Shao, Q.; Liu, P.; Xiong, L.; Wang, L.; Hong, X.; Xu, Y.; Wang, Z. Assessing the effects of adaptation measures on optimal water resources allocation under varied water availability conditions. *J. Hydrol.* **2018**, *556*, 759–774. [CrossRef]
- 33. Shen, Y.; Nielsen, K.; Revel, M.; Liu, D.; Yamazaki, D. Res-CN (Reservoir dataset in China): Hydrometeorological time series and landscape attributes across 3254 Chinese reservoirs. *Earth Syst. Sci. Data* 2023, 15, 2781–2808. [CrossRef]
- 34. Shen, Y.; Liu, D.; Jiang, L.; Tøttrup, C.; Druce, D.; Yin, J.; Nielsen, K.; Bauer-Gottwein, P.; Wang, J.; Zhao, X. Estimating reservoir release using multi-source satellite datasets and hydrological modeling techniques. *Remote Sens.* **2022**, *14*, 815. [CrossRef]
- 35. Yamazaki, D.; Ikeshima, D.; Sosa, J.; Bates, P.D.; Allen, G.; Pavelsky, T. MERIT Hydro: A high-resolution global hydrography map based on latest topography datasets. *Water Resour. Res.* **2019**, *55*, WR024873. [CrossRef]
- 36. Lehner, B.; Liermann, C.R.; Revenga, C.; Vörösmarty, C.; Fekete, B.; Crouzet, P.; Döll, P.; Endejan, M.; Frenken, K.; Magome, J.; et al. High-resolution mapping of the world's reservoirs and dams for sustainable river-flow management. *Front. Ecol. Environ.* **2011**, *9*, 494–502. [CrossRef]
- 37. Revel, M.; Zhou, X.; Yamazaki, D.; Kanae, S. Assimilation of transformed water surface elevation to improve river discharge estimation in a continental-scale river. *Hydrol. Earth Syst. Sci.* **2023**, *27*, 647–671. [CrossRef]

Water **2024**, 16, 2927

38. Kusumah, R.M.Y.P.; Abdurohman, M.; Putrada, A.G. Basement Flood Control with Adaptive Neuro Fuzzy Inference System Using Ultrasonic Sensor. *Int. J. Inf. Commun. Technol.* (*IJoICT*) **2020**, *5*, 11–19. [CrossRef]

39. Nurpambudi, R.; Wulandari, E.S.P.; Aziz, R.Z.A. Prediction of flood events in the city of Bandar Lampung using the artificial neural network. *J. Infotel* **2023**, *15*, 34–45. [CrossRef]

Disclaimer/Publisher's Note: The statements, opinions and data contained in all publications are solely those of the individual author(s) and contributor(s) and not of MDPI and/or the editor(s). MDPI and/or the editor(s) disclaim responsibility for any injury to people or property resulting from any ideas, methods, instructions or products referred to in the content.